# Two-Component LDV Investigation of Three-Dimensional Shock/Turbulent Boundary-Layer Interactions

J. D. Brown,* J. L. Brown,† and M. I. Kussoy†
*NASA Ames Research Center, Moffett Field, California*
M. Holt‡
*University of California, Berkeley, California*
and
C. C. Horstman†
*NASA Ames Research Center, Moffett Field, California*

**Mean velocity and turbulence measurements obtained by two-component laser Doppler velocimetry are presented, together with numerical predictions, for the shock-related separation of a turbulent boundary layer at Mach 2.85. The basic geometry—a 30 deg half-angle conical flare mounted on a long cylinder—is made three-dimensional by inclining the cone axis to the cylinder axis at an angle $\alpha$. Cases studied include $\alpha$ of 0, 5, and 10 deg. The separation length and general upstream influence increase with $\alpha$. A large-scale shock wave unsteadiness grows in amplitude with $\alpha$ and influences the amplification of turbulence correlations ahead of detachment. Scaling of the streamwise coordinate by separation length causes two- and three-dimensional data profiles on the cylinder to collapse for most measured quantities. The computed Navier-Stokes solutions show significant quantitative and qualitative departures from the data.**

## Nomenclature

| | |
|---|---|
| $d$ | = distance |
| $k$ | = two-dimensional turbulent kinetic energy, $k = 0.75(\overline{u'^2} + \overline{v'^2})$ |
| $M$ | = Mach number |
| $p$ | = wall pressure |
| $Re$ | = Reynolds number |
| $T$ | = temperature |
| $u,v,w$ | = velocity components |
| $X$ | = normalized streamwise coordinate |
| $x,y,z$ | = streamwise, vertical, transverse coordinates |
| $\alpha$ | = flare inclination angle |
| $\delta$ | = boundary layer thickness ($0.99U_\infty$) |
| $\epsilon$ | = turbulent kinetic energy dissipation rate |
| $\rho$ | = density |
| $\phi$ | = azimuthal coordinate |

*Subscripts and Superscripts*

| | |
|---|---|
| max | = maximum value |
| sep | = of separation |
| $t$ | = initial total condition |
| $w$ | = value at the wall |
| 0 | = value in the undisturbed boundary layer |
| $\infty$ | = value in the freestream |
| $\bar{(\ )}$ | = mean, ensemble-averaged quantity |
| $(\ )'$ | = fluctuating quantity |

Received Jan. 2, 1987; presented as Paper 87-0553 at the AIAA 25th Aerospace Sciences Meeting, Reno, NV, Jan. 12–15, 1987; revision received May 12, 1987. 

*NRC Research Associate.
†Research Scientist
‡Professor of Mechanical Engineering.

## Introduction

In the high-speed flows of practical interest, shock waves, three-dimensional effects, and large-scale separation of turbulent boundary layers are all common. A greater, more detailed physical understanding of these phenomena is presently needed to compliment huge recent advances in computational fluid dynamics (CFD) in working toward efficient and reliable design-caliber computations for aerodynamic applications. While numerous studies have been conducted on strong shock-wave/boundary-layer interactions (Ref. 1 gives a fairly comprehensive bibliography), a relative few report critical flowfield data, such as turbulent stresses and kinetic energies.

This paper presents mean surface pressures as well as flowfield velocity and turbulence data for a strong shock/boundary-layer interaction, at Mach 2.85, in which an axisymmetric geometry is made increasingly three-dimensional. Numerical solutions to the Reynolds-averaged Navier-Stokes equations are also compared with the data.

## Description of Experiment

Complete details of the experimental setup and procedures have been previously reported.[1] A summary is given here.

### Facility and Flow Model

The experiment was performed in the $25.4 \times 38.1$ cm rectangular test section of Ames Research Center's High Reynolds Number Channel I. Figure 1 shows the basic flow configuration and the coordinate system used. An equilibrium turbulent boundary layer forms over the 5.08 cm diameter stainless steel cylinder and is abruptly compressed as it approaches the 30 deg half-angle flare. When the flare is inclined, the interaction is three-dimensional. The cusped nose on the cylinder prevents formation of shocks that might otherwise reflect off the tunnel walls back to the model.

The principal region of study nominally extends five undisturbed boundary-layer thicknesses upstream of the compression corner and a similar distance downstream along the flare. The axisymmetric case, $\alpha = 0$ deg, and two three-

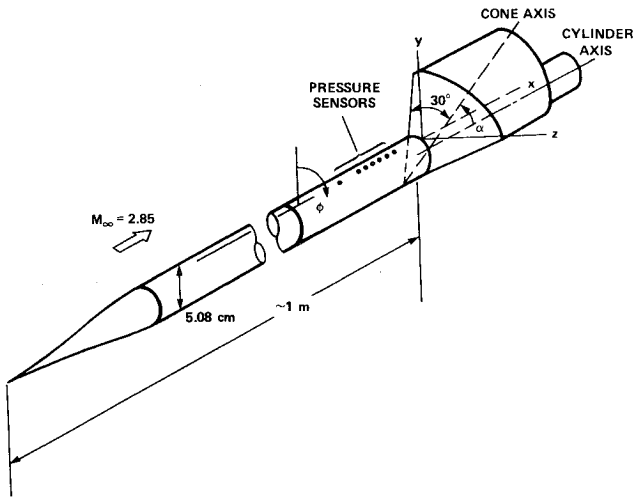


**Fig. 1 General flow configuration.**

dimensional configurations, $\alpha = 5$ and 10 deg, are examined. Data are presented for the upper symmetry plane, $z = \phi = 0$, only.

Nominal total and undisturbed flow conditions were: $T_t = 270$ K, $p_t = 1.7$ atm, $M_\infty = 2.85$, $Re = 16 \times 10^6$/m, and $\delta_0 = 1.1$ cm.

#### Surface Pressure Measurements

Mean wall pressures were measured through taps, 0.508 mm in diameter, spaced every 0.5 cm in the $\phi = 0$ deg plane, along both the cylinder and the flare. The estimated uncertainty of the pressure measurements is 5%.

A second cylinder, instrumented with six high-speed pressure transducers, was used during velocity measurements to record fluctuating wall pressures in the vicinity of separation. The pressures are used to examine large-scale shock unsteadiness, which is discussed below.

#### Velocity Measurements

Velocities were measured with a two-component laser Doppler velocimeter (LDV) operating in a two-color forward-scatter mode. Half-micrometer latex spheres were employed as light-scattering particles. A PDP 11/34 minicomputer was used for data acquisition and initial reduction. Most of the data analysis was performed on a VAX 11/780.

All ensemble averages were calculated from between 15,360 and 26,112 individual valid measurements, where the smaller number corresponds to lower data rates. The data rates depended on measurement location and ranged from approximately 1000 $s^{-1}$ (near separation) to 30,000 $s^{-1}$. The peak errors in the mean velocity and the turbulence quantities are estimated respectively at 5 and 15% of their maximum values. These are "worst cases" found at measurement locations with very high gradients; most of the data have lower uncertainties.

## Details of Navier-Stokes Solutions

The equations chosen to describe the mean flowfield were the time-dependent, Reynolds-averaged, Navier-Stokes equations for a three-dimensional fluid. For turbulence closure, the two-equation, $k$-$\epsilon$, eddy-viscosity model[2] with wall function boundary conditions[3] was used. The MacCormack, explicit second-order, predictor-corrector finite-volume numerical procedure[4] was employed.

The computational domain consisted of uniform mesh spacing in the streamwise and azimuthal directions. In the vertical direction, a geometrically stretched spacing was used near the solid surfaces, followed by a uniform spacing. The total mesh size was 64 points in the streamwise direction, 33 in the vertical direction, and 38 in the azimuthal. Typically, 16 mesh points were used to resolve the boundary layer.

The upstream boundary conditions were prescribed by a combination of uniform freestream conditions and the results of a boundary-layer computation matching the experimental displacement thickness. At the downstream boundary, the gradients of the flow variables in the streamwise direction were set to zero. In the azimuthal direction, symmetry conditions were applied at $\phi = 0$ and 180 deg. No-slip and constant wall temperature conditions were imposed at the surface where turbulent kinetic energy and dissipation were set to zero. The compressible two-dimensional wall functions derived in Ref. 3 were extended to three-dimensional flows by replacing the horizontal velocity with the total velocity parallel to the wall. The flow direction was also assumed to remain constant between the surface and the first grid point away from the surface. The $y^+$ location of the first grid point varied from 30 to 120.

## Results and Discussion

#### Mean Wall Pressures

Figure 2 shows the measured and computed streamwise wall pressure distributions for the three cases studied. Separation and reattachment locations estimated from mean velocity measurements are indicated. The initial measured pressure rise on the cylinder, a direct indication of the interaction's extent of influence, clearly moves upstream with $\alpha$, however, the computations do not reflect this trend.

#### Mean Velocity

Samples of measured and computed streamwise velocity profiles, on the cylinder and flare, appear in Fig. 3 for $\alpha = 0$ and 10 deg. The 5 deg case showed no exceptional behavior and is excluded. Again, the measurements clearly reflect the trend of increasing upstream influence with $\alpha$, while it is not as obvious in the computations. Mean boundary-layer detachment was estimated from the full set of measured profiles to occur at $x = -1.5$ cm for axisymmetric flow and $x = 2.5$ cm for $\alpha = 10$ deg. The corresponding computed values, based on vanishing skin friction, are $x = -0.5$ and $-1.38$ cm, respectively.

#### Turbulent Kinetic Energy

Figure 4 shows profiles of the two-dimensional turbulent kinetic energy on the cylinder and flare. It is noted that $k$ is the kinematic "kinetic energy" since the density is not included. Figure 5 plots the maximum measured kinetic energy, $k_{max}$, scaled by the maximum value in the incoming boundary layer, $k_{max(0)}$, at each streamwise location for all three cases studied.

The measurements show that $k$ is amplified substantially, prior to separation. The computations do not reflect this behavior. Figure 5 shows that the location of the first increase in $k_{max}$ moves upstream with increased $\alpha$, but that geometry has little effect on the magnitude of the overall rise.

#### Scaling

In Fig. 5, $k_{max}$ behaves similarly on the cylinder for all $\alpha$. The only large distinction is the $x$ location of the initial rise above the undisturbed value. This suggests that there might be a similarity between the cases if a proper scaling for the streamwise coordinate were chosen. Figure 6 plots kinetic energy profiles for all three flows, with $x$ scaled by the separation length as estimated from the mean velocity data; $y$ is scaled by local boundary-layer thickness. The measured profiles were interpolated in $x$ so they could be compared at the same locations.

The collapse of the data, particularly that of axisymmetric profiles onto the three dimensional, is striking. Profiles of $\overline{u'v'}$, $\overline{u'^2}$, mean velocities, and vorticity all respond similarly

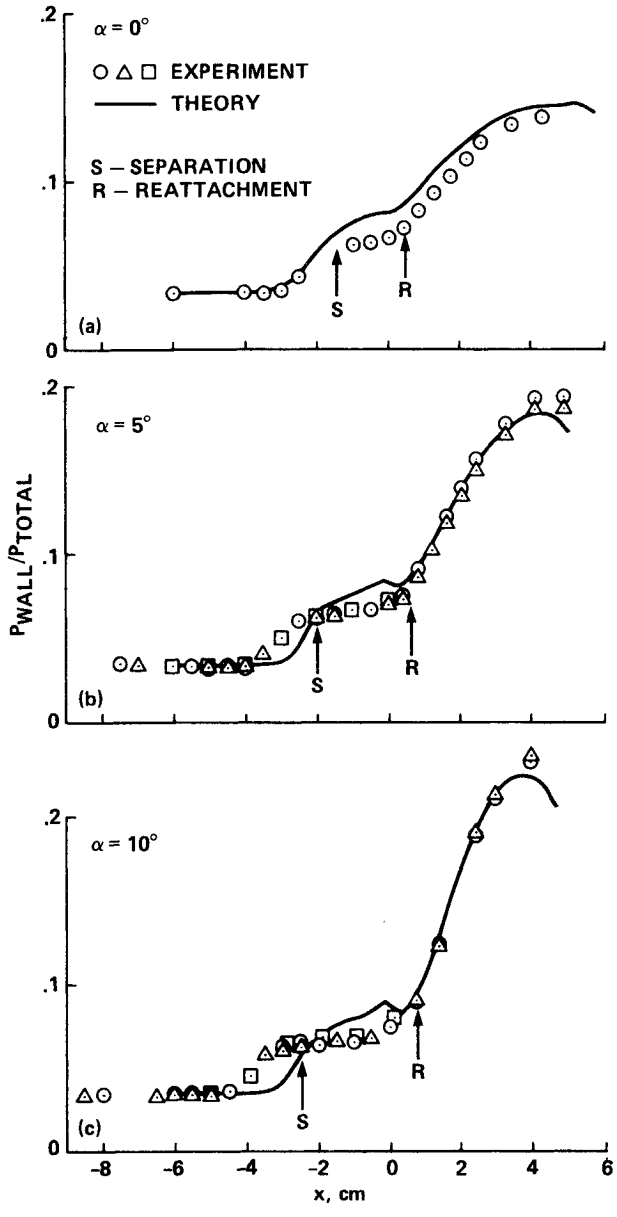


Fig. 2 Mean wall pressure.

to the scaling. The Navier-Stokes predictions exhibit no similar scaling.

The experimental results raise the prospect that, for certain flows, more easily obtained data on a two-dimensional geometry may provide valuable insight to a related three-dimensional case.

**Shock Unsteadiness**

It was previously reported[1,5,6] that the separation shock is unsteady in the current flow and undergoes large-scale (i.e., on the order of $\delta_0$), streamwise excursions that increase in amplitude with $\alpha$. Using high-speed-shadowgraph movies synchronized with instantaneous wall pressure measurements on the cylinder, a strong correlation was demonstrated (Fig. 7) between the shock motion and large intermittent wall pressure fluctuations at points upstream of separation. The quantity $d_s$ is the instantaneous distance from the compression corner of the separation shock at a fixed $y$ location, as determined from the shadowgraph movies; $d_{\Delta p}$ measures the distance from $x=0$ to the location on the cylinder where $p_w - p_{w(0)}$ is a selected constant. The constant values for $y$ and $\Delta p$ must be within the proper range to capture the shock motion and the large-amplitude pressure disturbances, but are otherwise arbitrary.

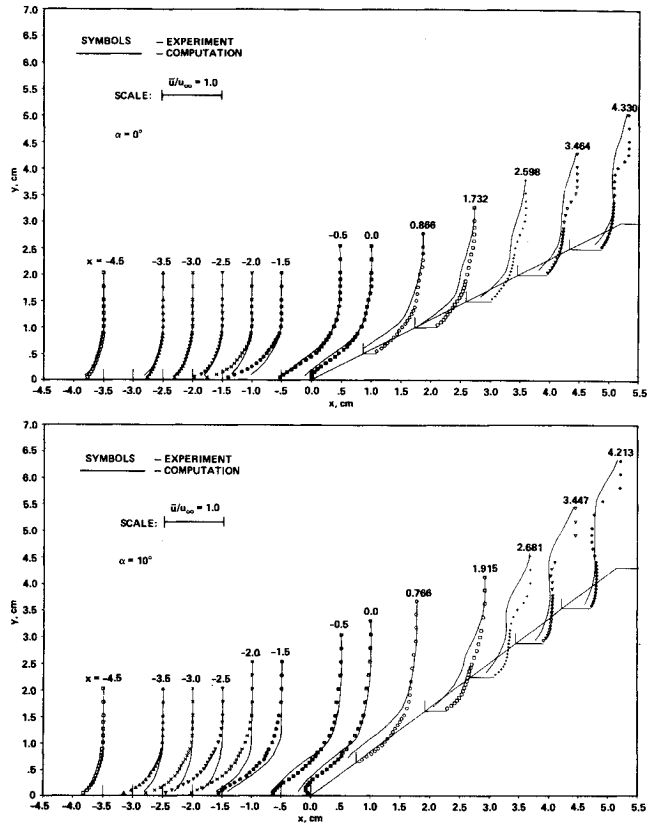


Fig. 3 Mean streamwise velocity profiles.

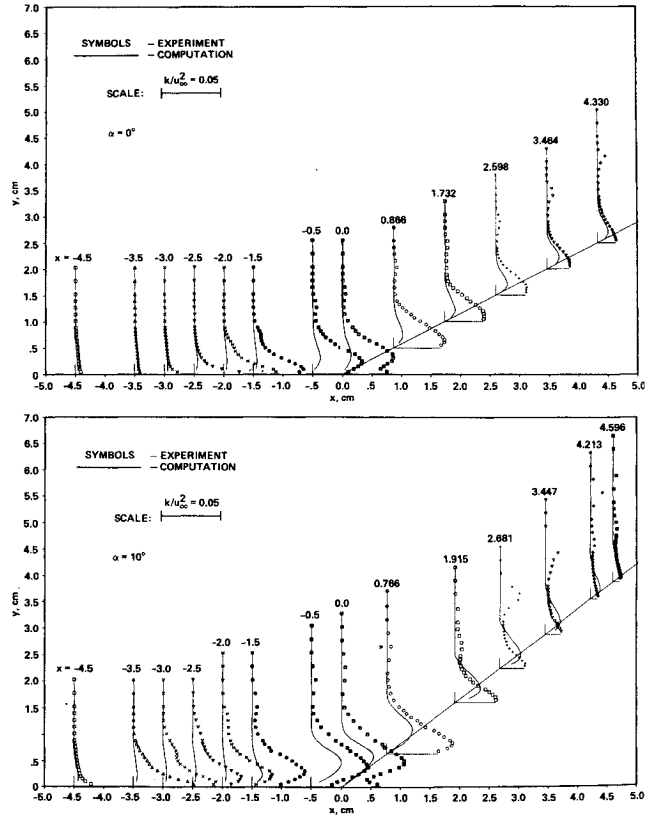


Fig. 4 Turbulent kinetic energy (two-dimensional) profiles.

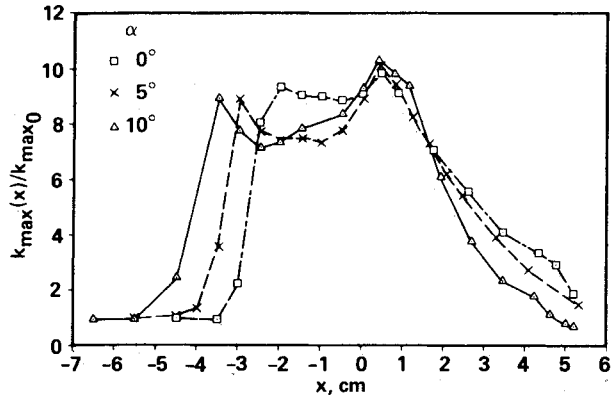


Fig. 5 Streamwise distribution of maximum turbulent kinetic energy.

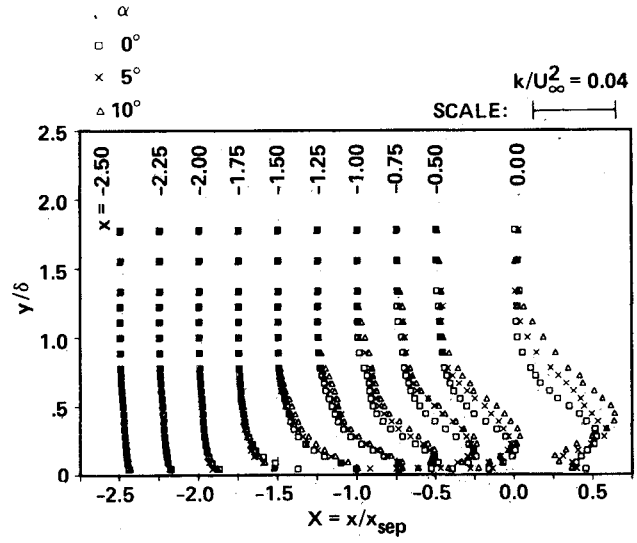


Fig. 6 Similarity of turbulent kinetic energy experimental profiles, streamwise scaling.

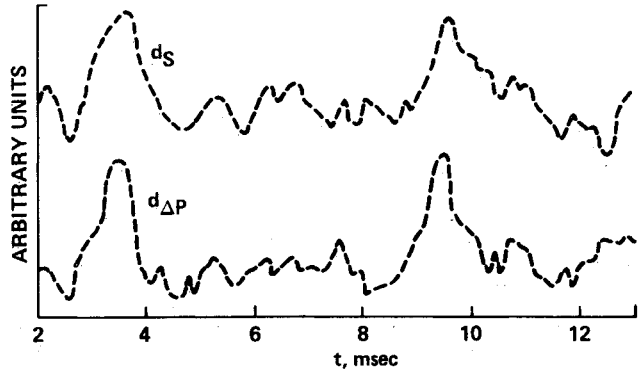


Fig. 7 Correlation of shock unsteadiness and wall pressure fluctuations.

The shock unsteadiness appears to affect measured turbulence correlations substantially. Figure 8 shows the existence of two peaks (see, for example, the profile at $x=-2.0$) in the kinematic shear stress for $\alpha=10$ deg. The

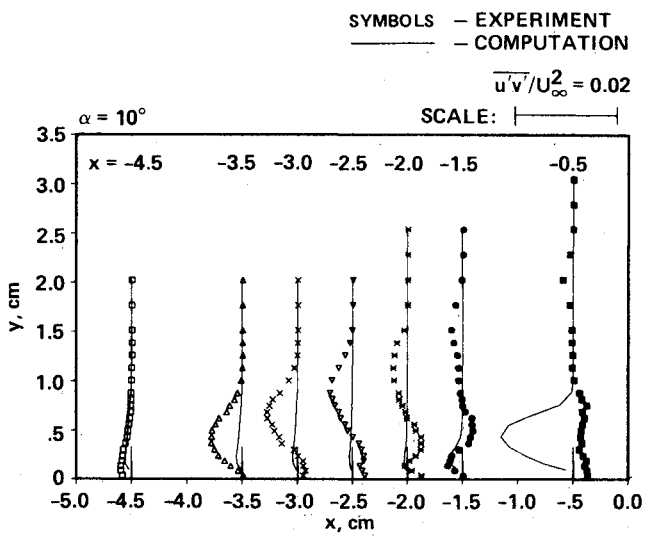


Fig. 8 Kinematic shear stress profiles.

larger, outer peak first appears near $x=-4.5$ cm, very close to the initial rise in rms wall pressure fluctuations. The smaller peak forms close to the mean separation point and corresponds to the detached shear layer. Shear stress profiles for $\alpha=5$ and 0 deg, cases that both exhibit shock unsteadiness, show the same behavior. However, for a 12 deg axisymmetric flare with no separation and a steady shock wave,[6] only a single peak appears.

The computations show the growth of only one shear stress peak, first amplified in the immediate vicinity of separation, which corresponds to the detached shear layer. No response of $\overline{u'v'}$ to unsteadiness is evident. This indicates a deficiency either in the numerics, the turbulence model, or both.

## Conclusions

The axisymmetric and three-dimensional separations of a Mach 2.85 turbulent boundary layer over a cylinder and flare have been studied. Mean wall pressure, velocity, and turbulence data, all measured in the upper symmetry plane, have been compared with results of Navier-Stokes computations in which a two-equation eddy-viscosity turbulence model was employed. The following major conclusions are drawn.

Upstream influence due to the compression, as gaged by initial disturbances in wall pressures, and mean and fluctuation velocities, increase with $\alpha$.

Scaling $x$ by mean separation distance causes the experimental data profiles on the cylinder for the different $\alpha$ values to collapse. The scaling works for most flow quantities. This raises the possibility that experimental and numerical investigations of certain three-dimensional separated flows might be simplified through the study of related two-dimensional geometries.

A large-scale shock unsteadiness, whose amplitude increases with $\alpha$, is observed in the flow. It is directly linked to significant growth in measured fluctuation levels in the upstream boundary layer.

The computed results exhibit significant quantitative and qualitative departures from the experiment. They show no case-to-case similarity when the streamwise coordinate is scaled, nor do they show any evidence of shock-wave unsteadiness, both key features of the measured data. Attempts to calculate the present flow with other combinations of numerical method and turbulence model appear to be warranted.

## References

[1]Brown, J. D., "Two-Component LDV Investigation of Shock-Related Turbulent Boundary Layer Separation with Increasing Three Dimensionality," Ph.D. Thesis, University of California, Berkeley, 1986.

[2]Jones, W. P. and Launder, B. E., "The Prediction of Laminarization with a Two-Equation Model of Turbulence," *International Journal of Heat and Mass Transfer*, Vol. 15, Feb. 1972, pp. 301-314.

[3]Viegas, J. R., Rubesin, M. W., and Horstman, C. C., "On the Use of Wall Functions as Boundary Conditions for Two-Dimensional Separated Compressible Flows," AIAA Paper 85-0180, 1985.

[4]MacCormack, R. W., "Numerical Solution of the Interaction of a Shock Wave with a Laminar Boundary Layer," *Lecture Notes in Physics*, Vol. 8, 1972, Springer-Verlag, Berlin, pp. 151-163.

[5]Horstman, C. C., Kussoy, M. I., and Lockman, W. K., "Computation of Three-Dimensional Shock Wave Turbulent Boundary Layer Interaction Flows," *Numerical and Physical Aspects of Aerodynamic Flows III*, Springer-Verlag, Berlin, 1986, Chap. 24.

[6]Brown, J. L., Kussoy, M. I., and Coakley, T. J., "Turbulent Properties of Axisymmetric Shock-Wave Boundary-Layer Interaction Flows," IUTAM Symposium on Turbulent Shear-Layer/Shock-Wave Interaction, Palaiseau, France, Sept. 9-12, 1985. *Turbulent Shear-Layer/Shock-Wave Interactions*, edited by J. Délerly, Springer-Verlag, Berlin, 1986, pp. 137-148.